Assessment of acid mist on mortar biodeterioration simulating the wall of Jardim da Princesa, the National Museum of Rio de Janeiro, Brazil

Diogo Simas, Bernardes Dias, Lizeth Y.A. Jaramillo, Douglas Guedes, Robert Duran, Anne Carbon, Luiz Bertolino, Ulrich Vasconcelos, Márcia T.S. Lutterbach, Eliana F.C. Sérvulo, Cristiana Cravo-Laureau

Assessment of acid mist on mortar biodeterioration simulating the wall of Jardim da Princesa, the National Museum of Rio de Janeiro, Brazil

Diogo S. B. Dias[*1a,b], Lizeth Y. A. Jaramillo[2a], Douglas Guedes[3a], Robert Duran[4b], Anne Carbon[5b], Luiz C. Bertolino[6c], Ulrich Vasconcelos[7d], Márcia T. S. Lutterbach[8e], Eliana F. C. Sérvulo[9a], Cristiana Cravo-Laureau[10b].

[a] Universidade Federal do Rio de Janeiro, Laboratório de Biocorrosão, Biodegradação e Biossíntese. Departamento de Engenharia Bioquímica, bloco E, Rua Athos da Silveira Ramos 149, Cidade Universitária, Ilha do Fundão, Rio de Janeiro - RJ, Brasil.

[b] Université de Pau et des Pays de l'Adour, Environmental Microbiology, CNRS UMR 5254 IPREM, E2S UPPA, 64000 Pau, France.

[c] Centro de Tecnologia Mineral – MCTI, Setor de Caracterização Tecnológica, Av. Pedro Calmon, 900. Cidade Universitária, Ilha do Fundão, Rio de Janeiro - RJ, Brasil.

[d] Universidade Federal da Paraíba, Laboratório de Microbiologia Ambiental, Centro de Biotecnologia, R. Ipê Amarelo s/n - Campus I, João Pessoa - PB, Brasil.

[e] Instituto Nacional de Tecnologia, Laboratório de Biocorrosão e Biodegradação, Divisão de Corrosão e Degradação, Avenida Venezuela, 82 – sala 616, Praça Mauá, Rio de Janeiro - RJ, Brasil.

[1*]Corresponding author - diogodias@eq.ufrj.br
[2] lizethacevedo@eq.ufrj.br
[3] douglas.guedes.ferreira@gmail.com
[4] robert.duran@univ-pau.fr
[5] anne.carbon@univ-pau.fr
[6] lcbertolino@cetem.gov.br
[7] u.vasconcelos@cbiotec.ufpb.br
[8] marcia.lutterbach@int.gov.br
[9] eliana@eq.ufrj.br
[10] cristiana.cravo-laureau@univ-pau.fr

ABSTRACT

This work aimed to evaluate the effect of acid mist on microbial communities developed on mortar with same composition from the wall of the National Museum in Rio de Janeiro. Five autochthonous microbial groups were inoculated on coated with acrylic paint and uncoated mortar surfaces and submitted to acid mist or water mist for 100 days. A heterogeneous biofilm was well developed in uncoated coupons under acid mist. Molecular analysis revealed that the bacterial communities were structured according to the incubation condition. The impact of coating on bacterial community structure was more important than the acid mist effect. The eukaryotic community structure was not affected by the acid mist, whereas the impact of coating by paint has been observed. The alpha diversity indexes also varied according to the treatment. H' and D were higher for uncoated conditions, particularly when submitted to acid mist. Actinobacteria, Chloroflexi, Cyanobacteria, Firmicutes and Proteobacteria were dominant. Additionally, eukaryotic community was not affected by the acid mist and paint and Tremellomycetes dominated.

Keywords: National Museum of Rio de Janeiro; bioreceptibility; biodeterioration; acid mist.

1 INTRODUCTION

Ancient and modern monuments are prone to deterioration caused by variable interaction of biotic and abiotic factors. They are composed by a wide range of materials of different texture and structure, features determining their ability to resist weathering (Miller et al., 2012, Mapelli et al., 2012; Saddique & Chahal, 2011; Sarró et al., 2006). The occurrence of biodeterioration in historical monuments is multifactorial and not fully understood because it is a multifactorial phenomenon that affect differently according to the type of materials, the location, and the colonization by microorganisms (Mihajlovski et al., 2017; Perez-Alvaro, 2016). Anthropogenic activities accelerate the biodeterioration processes by depositing organic pollutants on material surfaces that stimulates microbial growth (Manso et al., 2014; Saiz-Jimenez, 1995). In addition, abiotic conditions, such as marine spray and acid rain, also favor the microbial development increasing the deterioration of materials, including modern materials such as mortar (Traversetti et al., 2018; Shirakawa et al., 2010; Mitchell & Gu, 2000).

Bioreceptibility, concept proposed by Guillitte (1995), aims to characterize materials according to their ability to be colonized by microorganisms, providing useful information on the resistance of materials to biodeterioration. Several studies have characterized the bioreceptibility of construction materials such as stones (Nuhoglu et al., 2017), granite (Vásquez-Nion et al., 2018) or mortar (García-Esparza et al., 2017; Jurado et al., 2014), including both covered and uncovered surfaces (Shirakawa et al., 2011; Gaylarde et al., 2011). Cement based materials contain organic adjuvants increasing bioreceptibility, i.e. favoring the primary colonization by microorganisms involved in the biodeterioration process (De Muynck et al., 2009). However, further studies are required in order to evaluate the parameters influencing the microbial colonization and development dynamics in cements-based materials, knowledge of paramount importance for the implementation of preservation strategies (Wiktor et al., 2011; Reis-Menezes et al., 2011).

Regrettably, little attention has been devoted to the biodeterioration effects on Brazilian heritage monuments. Brazil, a 520-year-old country, own many historical monuments and cities that are strengthened by biodeterioration, particularly context of global changes (Gaylarde et al., 2018; Shirakawa et al., 2013; Lutterbach et al., 2013). The present work aimed to evaluate the biodeterioration process on material similar to that found in the walls of the Jardim da Princesa, located in the National Museum of Rio de

Janeiro (NM). In a perspective of preservation, the study examined the effect of acid mist on microbial colonization of mortar coated and uncoated coupons. We developed an experimental microbial ecology approach combining elemental and chemical analysis, imagery and biology tools, in order to follow microbial colonization and the effects on the construction materials. The gained information will be useful for the implementation of countermeasure for the preservation of Brazilian cultural heritage monuments.

2 MATERIALS AND METHODS

2.1 Site of study

The National Museum (NM), located in the Quinta da Boa Vista, São Cristóvão neighborhood, (22º 90 '57 "S, 43º 22' 65" W) is the oldest scientific institution in Brazil and the largest museum of natural history and anthropology in Latin America. It was created by King D. João, the 6th on June 6, 1818, serving as Residence of the Brazilian Imperial Family until 1889. The NM is located in an urban area, surrounded by heavy vehicle traffic. The place is well wooded, however, characterizing a zone that is usually very humid (60-70%).

2.2 Biomass collection

The samples were taken from two equidistant points on the northern wall of the Jardim da Princesa in the NM, by means of scraping, with a sterile scalpel (Medbisturi 23) and placed in penicillin bottle with 50 ml reducing solution, composed by NaCl 0.85 g/L, ascorbic acid 0.132 g/L and 4 mL of rezasurin solution 0.0025 g/L (Dias et al., 2016). Quantification of seven microbial groups were carried out as follows (Table S1): aerobic and facultative (not “strict anaerobe”) heterotrophic bacteria, aerobic and facultative acid producing bacteria, iron-oxidizing bacteria, filamentous fungi, and photosynthetic microorganisms, using spread plate and Most-Probable-Number (MPN) techniques (Genhardt et al., 1994). Significant differences between conditions were determined by analysis of variance (ANOVA).

2.3 Biodeterioration experiments

The assay was carried out in a glass reactor (Figure 1), measuring 60 cm wide x 30 cm deep x 40 cm high, was fitted with an artificial lighting system with two 60W tubular fluorescent lamps (Famastil). Fifty-six coupons similar to the composition of mortar

found in the wall of the NM were prepared with the mixture of sand (20 g), cement (30 g; commercial cement composed by tricalcium and dicalcium silicate, 10-70%; calcium iron-aluminate, 5-15%; calcium sulfate, 2-10%; tricalcium aluminate, 1-15%; calcium carbonate, 0-5%; magnesium oxide, 0-4%; calcium oxide, 0-0.2%), clay (5 g) and distilled water (13 mL). The coupons were molded into rectangles (4.0 cm long x 2.0 cm wide x 1.0 cm high) and cylinders (1.5 cm in diameter x 1.0 cm in height). Half of the coupons were coated with commercial acrylic paint (Coral, Rio de Janeiro, Brazil).

Biofilm development on the coupons was investigated in triplicate over 100 days (28°C±3°C and humidity ranged 30-50%), under 8 conditions (Table S2, Condition 1-CUW: Absence of microorganism, uncoated coupons and water mist; Condition 2-CCW: Absence of microorganism, coated coupons and water mist; Condition 3-CUA: Absence of microorganism, uncoated coupons and acid mist; Condition 4-CCA: Absence of microorganism, coated coupons and acid mist; Condition 5-MUW: Presence of microorganism, uncoated coupons and water mist; Condition 6-MCW: Presence of microorganism, coated coupons and water mist; Condition 7-MUA: Presence of microorganism, uncoated coupons and acid mist; Condition 8-MCA: Presence of microorganism, coated coupons and acid mist).

The inocula (50 mL) corresponded of a consortium prepared by mixing equal volumes of suspensions of five isolated groups from the wall samples: aerobic heterotrophic bacteria (10^{10} CFU/mL), anaerobic heterotrophic bacteria (10^{8} cells/mL), iron-oxidizing bacteria (10^{8} CFU/mL), total fungi (10^{6} CFU/mL) and photosynthetic organisms (10^{5} Cells/mL). The consortium was inoculated on the coupon surface at a rate of 0.25 mL/cm^2 in 3 applications at day 0, 7 and 14.

In order to monitor the climatic conditions of the system, a hygrometer (INCOTERM®) was used, and a humidifier (Multitoc Health) coupled with a thermostat (ATMAN, AT-100) were used to humidify the system. In order to simulate the composition of rainfall in the city of Rio de Janeiro, an acid mist was prepared containing: $NaNO_3$ (1607 µg/L), $CaSO_4.2H_2O$ (5281 µg/L), K_2SO_4 (1570 µg/L), NH_4Cl (1118 µg/L), NaCl (3680 µg/L), NaOH (212 µg/L), pH 5.12 (Hernández et al., 2010). The control mist was made with sterilized distilled water, pH = 6,0 ± 0,5.

Microbial quantification was carried out in the one hundred day of incubation. Aerobic heterotrophic bacteria, iron-oxidizing bacteria and total fungi were determined using spread plate technique and photosynthetic microorganisms, facultative heterotrophic

bacteria, aerobic and facultative acid producing bacteria were estimated using MPN technique.

2.4 Composition and structure of materials by X-Ray Fluorescence (XRF) and Scanning Electron Microscopy (SEM)

The oxides composition of the wall and coupons were determined by X-ray fluorescence (XRF) spectrophotometry (WDS, AXIOS Panalytical). Both samples, from wall and coupons were prepared in a VANEOX automatic press (20 mm mold, P = 20 ton and t = 30s), using boric acid 1:0.5 (2 g of the sample to 1.0 g of boric acid) as binder. The results are semi-quantitative expressed in %, calculated as 100% standardized oxides. The determination of the loss by calcination (LBC) of the samples was done in Leco TGA-701 equipment. First heating ramp 10°C/min at 25-107°C (for moisture removal), second ramp 40°C/min at 107-1000°C (for LBC determination). The test was completed after 3 identical weighing sequences. The measurement was performed under normal air conditions.

The images of the coupons were performed by Scanning Electron Microscopy (SEM, TM3030 PLUS). The samples had been previously metallized with gold/carbon with argon as the entrainment gas, using BAL-TEC (SCD 005, Sputter Coater), with a 30 mA current for 150 seconds under pressure between 10^1-10^2 Bar.

2.5 Microbial molecular analysis

2.5.1 DNA extraction

Biofilm samples for molecular analysis were collected from coupons, using sterile scalpel, and suspended in 50 mL sterile reducing solution (NaCl 0.85 g/L, ascorbic acid 0.132 g/L and 4 mL/L of rezasurin solution at 0.0025 g/L) in Penicillin bottles. 10 mL of solution was filtered through a membrane (0.2 µm Supor® Membrane, Microfunnel Filter Unit, Life Sciences). Membranes were cut before DNA extraction using UltraClean Soil DNA Isolation Kit (MOBIO) according to the manufcturer's instructions.

2.5.2 DNA amplification, purification and Terminal Restriction Fragment Lenght Polymorphism (T-RFLP) analyses

16S rRNA genes were amplified using Bacteria primers 63F (5′-CAGGCCTAACACATGCAAGTC-3′) and 1387R (5′-GGGCGGWGTGTACAAGGC-

3′) (Marchesi, et al., 1998). 18S rRNA genes were amplified using universal eukaryotic primers Euk1 (5′-CTGGTTGATCCTGCCAG-3′) and Euk516R (5′-ACCAGACTTGCCCTCC-3′) (Sogin & Gunderson, 1987). The reaction mix (25 µL final volume) contained 12.5 µL of AmpliTaq Gold 360 Master Mix 2x (Life Technologies), 0.2 µM of each primer and 5 µL of DNA template. PCR conditions were as follows: initial denaturation (95°C for 10 min) followed by 35 cycles of denaturation (95°C for 30 s), annealing (58°C for 45 s for Bacteria 16S rRNA; 56°C for 45 s for 18S rRNA gene) and extension (72°C for 1 min). PCR products were purified using an Illustra GFX 96 PCR Purification Kit (GE Healthcare) and digested with 3 U of Alu1 and Rsa1 (New England Biolabs) for 16S rRNA and with 3 U of Alu1 and HaeIII (New England Biolabs) for 18S rRNA, in a total volume of 10 µL at 37 °C for 3 h. T-RFLP analysis was performed as previously described (Stauffert et al., 2009). Datasets were constructed using a minimum peak height of 100 fluorescence units. T-RFLP profiles were aligned by identifying and grouping homologous fragments and normalized by calculating relative abundances of each terminal restriction fragment (T-RFs) from height fluorescence intensity, using T-REX software (Culman et al., 2009).

In order to compare bacterial and eukaryotic communities (T-RFLP patterns data) according to treatment and time, two-dimension nonmetric multidimensional scaling ordination (NMDS) based on Bray–Curtis distances was performed using Primer 6 software (Primer E, Plymouth, UK software). The significant differences between groups were tested with an analysis of similarities (ANOSIM) and similarity percentages test (SIMPER) performed with Primer 6.

2.5.3 High-throughput sequencing and data analysis

The bacterial and eukaryotic diversity of 36 samples was analyzed by Illumina MiSeq sequencing. MiSeq sequencing was performed at the GeT platform (Toulouse, France). The primers used were 104F (GGCGVACGGGTGAGTAA) (Wang & Qian, 2009) and 530R (CCGCNGCNGCTGGCAC) (Weisburg et al., 1991) for amplification of 16S rRNA gene, and EUK1A (CTGGTTGATCCTGCCAG) and 516R (ACCAGACTTGCCCTCC) (Sogin & Gunderson, 1987) for amplification of 18S rRNA gene. PCR conditions included10-min heating step at 95 °C followed by 30 cycles of 95°C - 30 s, 568°C - 30 s, 72°C - 45 s, and final extension at 72°C for 10 min for Bacteria and 10 min heating step at 95°C followed by 35 Cycles of 95°C - 45 s, 56°C - 45 s, 72°C - 1 min, and final extension at 72°C for 10 min for Eukaryote.

QIIME2 software (Quantitative Insights Into Microbial Ecology) was used to analyze gene sequence reading of 16S rRNA and 18S rRNA (Bolyen et al., 2018). The taxonomy assignment (97% similarity) was performed comparing reference sequences to SILVA (v132) database of known 16S and 18S rRNA genes (Quast et al., 2013). The alpha-diversity analysis (Shannon-Weaver, Simpson, Pielou's eveness and Good's coverage) was performed on rarefied count data using the apha_diversity.py script in Qiime2. Differential analysis and barplots were performed with SHAMAN (SHiny application for Metagenomic Analysis, shaman.c3bi.pasteur.fr) (Quereda et al., 2013). The complete dataset was deposited in the NCBI Sequence Read Archive (SRA) database (SUB7892718). It is available under the Bioproject ID PRJNA655939.

3 RESULTS

3.1 Characterization of coupons and wall

The composition of coupons was similar to that of the National museum (NM) wall, with the same composition of nine oxides (Table S3), with only a difference in the percentage of Al_2O_3.

3.2 Characterization of biodeterioration

The impact of biodeterioration on the surface of the coupons and the formed biofilm were characterized by SEM observations after 100 days of incubation (Figure 2). The coated surfaces (conditions 2-CCW, and 4-CCA) showed smoother surfaces than uncoated conditions (conditions 1-CUW and 3-CUA), which presented roughness and deposits of inorganic and organic matter, dust and other debris (Figure 2). Noteworthy, hyphae were observed in uncoated condition treated with acid mist (condition 7-MUA) associated with the greenish and orange color as shown in Figure 3 and observed by optical microscopy (data not shown), probably due to the development of photosynthetic microorganisms and by the activity of iron-oxidizing bacteria, respectively.

Biofilms of coated conditions were less dense compared to the uncoated coupons (conditions 5-MUW and 7-MUA). In addition, the coupons in condition 5 (MUW) showed the bulkier structure and less adherent than coupons in condition 7 (MUA). The presence of microorganisms altered the porosity of the material, as revealed by grooves observed in the surface of coupons. The coated coupons submitted to water mist (condition 6-MCW) presented depigmentation, despite the lower microbial

development. Cracks were observed in the surface of coated coupons (conditions 6-MCW and 8-MCA), suggesting microbial activity.

After scraping off the biofilms, coated coupons presented more visual alterations than uncoated coupons, with numerous spots over all the surface. In addition, whitening was observed in the coupons exposed to acid mist (condition 8-MCA), suggesting growth of fungal mycelium and/or presence of iron-oxidizing bacteria. On the other hand, the color of the paint changed to bright yellow, quite different from the coupons not exposed to the acid mist (condition 6-MCW).

The description of deterioration aspects and the quantification of microbial groups are summarized in Table 1. Under all inoculated tested conditions, heterotrophic bacteria were dominant, with a prevalence of aerobic communities. Also, the numbers of aerobic acid producing bacteria were similar under all conditions, with values around 10^2 cells/cm^2. The largest biomass was observed on the uncoated coupons (conditions 5-MUW and 7-MUA). The paint was not inhibiting microbial growth, except that of the facultative acid-producing and photosynthetic microorganisms (conditions 6-MCW and 8-MCA) for which the number of cells/cm^2 was reduced by at least 10^3 units (cells/cm^2) in comparison to the uncoated coupons (ANOVA, p-value < 0.001) irrespective of the atmospheric treatment (Table 1, conditions 5-MUW and 7-MUA). The presence of coating (condition 6-MCW) inhibited also the development of the iron-oxidizing bacteria (10^3 cells/cm^2, Table 1) (ANOVA, p-value < 0.001) and the total fungi (10^3 CFU/cm^2) (ANOVA, p-value < 0.001) but the inhibition effect was suppressed in presence of acid mist (condition 8-MCA).

3.3 Microbial communities structure and composition

Bacterial and eukaryotic community structures were monitored by T-RFLP based on 16S and 18S rRNA genes analyses for all incubation conditions at the end of the experiment (Figure 4). The T-RFLP analysis revealed that the bacterial communities were structured according to the incubation condition after 100 days of incubation (Figure 4A), the impact of coating (ANOSIM R= 0.833) on bacterial community structure was more important than the acid mist effect (R=0.289). The eukaryotic community structure (Figure 4B) was not affected by the acid mist (R=0.130), whereas the impact of coating by paint (R=0.389) has been observed. These results suggest that paint coating contributed to the selection of specific microbial species resulting in the dominance of some microbial groups.

In order to determine the impact of coating and acid mist on the microbial assemblages in the biofilms developed in coupons, bacterial and fungal communities composition were characterized by high throughput sequencing of 16S and 18S rRNA genes respectively. For bacterial community analysis, a total of 485567 16S rRNA gene reads were obtained for the 12 samples. The obtained valid reads after preprocess filtering and normalization were reduced to 6983 sequences for each sample, clustered into 126 amplicon sequence variants (ASVs). For eukaryotic community, 267103 18S rRNA gene reads were obtained. After filtering and normalization, and focusing only in Fungi, 4599 sequences were obtained for each sample, clustered into 23 ASVs. Good‘s coverage values, nearly 100% in each sample, indicated that the main bacterial and fungal diversity were assessed.

The alpha diversity indexes [Shannon (H’), Simpson (D) and equitability] varied according to the treatment for bacterial and fungal communities (Table 4). H’ and D were higher for uncoated conditions, particularly when submitted to acid mist. Furthermore, microbial communities from coated conditions were dominated by some microorganisms, as indicated by equitability index (Pielou’s eveness).

The dataset consisted of 5 distinct bacterial phyla: Actinobacteria, Chloroflexi, Cyanobacteria, Firmicutes and Proteobacteria. Among the most abundant genus in uncoated coupons with water mist (condition 5-MUW, Figure 5A), *Microbacterium* was the most abundant (comprising 40.1 % of the classified community), followed by *Brevundimonas* (34.9 %), *Roseomonas* (10.6 %), *Skermanella* (6.5 %) and *Methylobacterium* (4.5 %). In uncoated coupons submitted to acid mist (condition 7-MUA) a modification of the bacterial community composition was observed (Fig. 5A) showing the dominance of Cyanobacteria belonging to *Leptolyngbya* (38.8 %) and *Nostoc* (5.4 %) genus. A decrease of the abundance of *Microbacterium* (6.7 %) and the detection of *Micromonospora* (7.6 %), both belonging to Actinobacteria, was also observed. Proteobacteria dominated the bacterial communities of coated coupons (conditions 7-MUA and 8-MCA), with *Methylobacterium* (Fig. 5A) as the most abundant genus in both water and acid mist conditions (conditions 7-MUA and 8-MCA, 81.2 % and 91.1 % respectively).

Fungal communities were represented by two phyla, Ascomycota and Basidiomycota. Uncoated coupons (conditions 5-MUW and 7-MUA) were dominated by the class Tremellomycetes (68.8 % and 69.8 % respectively) followed by Sordariomycetes (31.2 % and 30.1 % respectively) irrespective of the mist condition (Figure 5B). Coated

coupons (conditions 6-MCW and 8-MCA, Figure 5B) were dominated by Sordariomycetes (97.3 % and 89.4 % respectively). At the ASVs level, for the two fungal dominant classes (Figure 5C), data analysis showed that conditions (coat and mist) had an impact on the distribution of ASVs abundances but not on the composition.

4 DISCUSSION

4.1 Biodeterioration of mortar

The composition of coupons was overall similar to that of the National museum (NM) wall supporting that coupons can be used to simulate NM wall. However, a difference in the aluminium oxide content was observed. Aluminium toxic effects on microorganisms has been showed (Piña & Cerventes, 1996) as well as tolerance capacities (Piotrowska-Seget et al, 2005; Ahmed et al, 2020). The concentration of Al_2O_3 observed in the NM wall (400 ppm) can be considered as high and inhibitory for microbial growth (Piña & Cerventes, 1996). This suggests that microorganisms colonizing the wall are tolerant and able to be adapted and grow in the coupons, result obtained in the present study support this hypothesis. Moreover, calcination loss showed differences, probably due to the presence of organic matter on the wall from the paint, and/or microorganisms, exopolysaccharides and other particles deposited by wind and rain (Hartmann et al., 2014).

The impact of biodeterioration of mortar samples was greater on the surface in uncoated coupons than on the coated coupons. The uncoated coupons were more susceptible to bioreceptibility due to their structural features that favor microbial development as previously described (Silva et al., 2019; Viana et al., 2017).

In addition, the uncoated coupons also showed thicker biofilm and microbial morphological diversity, showing heterogeneous development, compared to the coated coupons, suggesting the influence of paint on microbial growth and biofilm development, without complete inhibition. These observations are in agreement with several studies showing that external painted surfaces support a diverse microbial population (for review, see Gaylarde et al., 2011). Furthermore, a previous study showed that microbial activity had promoted material surface deterioration, resulting in an increase in the porosity and a decrease in its resistance and subsequent crumbling (Papida et al., 2000), as well as desquamation was reported as result of volume change, matrix penetration and release of microbial metabolites such as organic and inorganic acids (Coutinho et al., 2013).

The positive effect of acid mist on the biofilm adhesion has been observed irrespective of the presence of paint, suggesting that acid mist promote microbial growth and consequently, material biodeterioration. These observations corroborate the hypothesis that acid mist causes more damage to the material than humidity caused by the water mist, because it keeps the surface moister beyond the acids act on surface deterioration. These observations are in accordance with a study that demonstrated the impact of atmospheric conditions on the degree of material deterioration (Gil et al., 2010). Additionally, microbial influence was greater than that of the atmosphere in the process of surface deterioration, due to production of acids and other metabolites (Pitzurra et al., 2003).

The results of microbial quantification are consistent with the SEM observations that showed a larger biofilm development on uncoated coupons. It has been reported that the paint on materials (coated) impact in microbial growth (Gaylarde et al., 2011). Most of microorganisms in our study have not been totally inhibited, in the exception of photosynthetic microorganisms (condition 6-MCW). This observation was in contradiction with several studies that reported the presence of Cyanobacteria on painted surface, particularly in tropical and subtropical countries (Shirakawa et al., 2011; Gaylarde & Gaylarde, 1999). It was also reported that fungi constitute the major biomass on painted surfaces in Latin America (Gaylarde & Gaylarde, 2005).

It is important to highlight that the presence of acrylic paint (condition 6-MCW) also inhibited the development of two groups: iron-oxidizing bacteria and the total fungi and the inhibition effect was suppressed in the presence of acid mist (condition 8-MCA). Overall, the acid mist has favored microbial development, especially on the coated coupons (Table 1, condition 5-MUW vs condition 7-MUA and condition 6-MCW vs condition 8-MCA). The same observation was previously demonstrated by some studies (Flemming & Wingender (2001), Costerton et al. (1995).

4.2 Microbial communities structure and composition

The culture-based approach used in the present study allow to obtain diverse microbial communities in the different conditions. The composition of these microbial communities is representative of the microbial community observed *in situ* (data not shown). Indeed, the *in situ* community was mainly dominated by Cyanobacteria (46%, relative abundance), Proteobacteria (20%, relative abundance) and Actinobacteria (17%, relative abundance), also observed as main bacterial phyla in coupons from the

biodeterioration experiment. The fungal *in situ* community was dominated by the phylum Basidiomycota, as observed in coated coupons. The comparison of environmental and culture-derived microbial communities showed that the diversity of culture-derived communities reflected selectivity of the culture media and/or the culture condition, as previously described (Pédron et al., 2020).

The five phyla observed in the present study have been found dominant in recent works evaluating the biodeterioration of cultural heritage monuments (Lepinay et al., 2018; Adamiak et al., 2018; Chimienti et al., 2016). Among these phyla, Actinobacteria have been identified as dominant in biofilms of historic monuments (Adamiak et al., 2018; Mihajlovski et al., 2017). It is well known that they inhabit more effectively stone and mural paintings, by their ability to use various nitrogen and carbon sources (Sterflinger et al., 2013). Surprisingly, in the present study these microorganisms were impacted by the acid mist. In fact, these microorganisms are known to play a crucial role in the decomposition of organic compounds and environmental pollutants, and thus expected to resist and adapt to the acid mist. It is a premise that the atmospheric condition inhibits both the size and diversity of the biofilm microbial community (Mitchell & Gu, 2000).
The acid mist promoted the development of Cyanobacteria on uncoated coupons. Cyanobacteria are known to support the growth of heterotrophic bacteria and fungi by being a nutrient source, thus constituting a key element in the biofilm formation and maintenance. Cyanobacteria have been described to be involved in biodeterioration of cultural heritage monuments (Dyda et al., 2018; Herrera & Videla, 2004) and to be dominant in biofilms in different climatic sites (Gaylarde & Gaylarde, 2005). Additionally, Proteobacteria dominated the bacterial communities of coated coupons, indicating their resistance to coating and supporting their implication on material biodeterioration (Lepinay et al., 2018; Mihajlovski et al., 2017; Jurado et al., 2014).
Concerning fungal diversity, the uncoated coupons were dominated by Tremellomycetes and Sordariomycetes, whereas coated coupons were dominated by Sordariomycetes. These observations suggested that fungi affiliated to this class are adapted to the presence of paint. Our results also support the impact of paint and acid mist in the fungal community composition (e.g. TRFLP analysis, Figure 4B) showing stronger impact of paint than acid mist in the fungal community composition. Fungi affiliated to the Sordariomycetes class have been identified as common colonizers of paint biofilms in Brazil (Shirakawa et al., 2010; Shirakawa et al., 2002) and recently

identified in mortar coatings of a historical building (Guerra et al., 2019). Furthermore, they have been described as involved in concrete deterioration (Wei et al., 2013).

The use of paint reduced the fungal population. Some antimicrobial additives found in paints, such as titanium dioxide (Amorim et al., 2020), zinc pyrithione (Reeder et al., 2011), ammonium-aqueous solution, ethane 1,2-diol and kaolin (Chukwujike and Igwe, 2019) act to prevent fungal adsorption and consequently avoid the establishment of biofilm. The paint used in the present work, one of the most sold in Brazil, is composed by antifungal, antialgal and antibacterial additives, according to manufacturers.

5 CONCLUSIONS

Our results indicated that microbial deterioration will always occur, even at different degrees, irrespective of the coating and moisture condition. The experimental approach applied in the present work is proposed as a strategy to address bioreceptibility. This approach has the advantage to be less time-consuming than *in situ* studies, not destructive, using lab controlled systems with the possibility of extrapolation to the real ecosystem.

ACKNOWLEDGEMENTS

The English text of this paper has been revised by Sidney Pratt, Canadian, MAT (The Johns Hopkins University), RSAdip - TESL (Cambridge University).

FORMATTING OF FUNDING SOURCES

This work was supported by the Conselho Nacional de Desenvolvimento Científico e Tecnológico (CNPq); and Coordenação de Aperfeiçoamento de Pessoal de Nível Superior (CAPES - Fellowship Program number 99999.008278/2014-08).

REFERENCES

Adamiak, J., Otlewska, A., Tafer, H., Lopandic, K., Gutarowska, B., Sterfinger, K., Piñar, G., (2018). First evaluation of the microbiome of built cultural heritage by using the Ion Torrent next generation sequencing platform. *International Biodeterioration & Biodegradation*, 131, 11-18. https://doi.org/10.1016/j.ibiod.2017.01.040.

461 Ahmed B., Ameen F., Rizvi A., Ali K., Sonbol H., Zaidi A., Khan M.S., Musarrat J.,
462 (2020) Destruction of Cell Topography, Morphology, Membrane, Inhibition of
463 Respiration, Biofilm Formation, and Bioactive Molecule Production by Nanoparticles
464 of Ag, ZnO, CuO, TiO2, and Al2O3 toward Beneficial Soil Bacteria, *ACS Omega,*. 5,
465 7861–7876. https://doi.org/10.1021/acsomega.9b04084.

466

467 Amorim, S. M., Sapatieri, J. C., Moritz, D. E., Domenico, M., Laqua, L. A.C., Moura-
468 Nickel, C. D., Aragão, G. M. F., Moreira, R. F. P. M. (2019). Antifungal and
469 photocatalytic activity of smart paint containing porous microspheres of TiO2.
470 *Materials Research*, 22, e20190470. https://doi.org/10.1590/1980-5373-mr-2019-0470.

471

472 Bolyen, E., Rideout, J. R., Dillon, M. R., Bokulich, N. A., Abnet, C., Al-Ghalith, G. A.,
473 Alexander, H., Alm, E. J., Arumugam, M., Asnicar, F., Bai, Y., Bisanz, J. E., Bittinger,
474 K., Brejnrod, A., Brislawn, C. J., Brown, C. T., Callahan, B. J., Caraballo-Rodríguez, A.
475 M., Chase, J., Cope, E., Da Silva, R., Dorrestein, P. C., Douglas, G. M., Durall, D. M.,
476 Duvallet, C., Edwardson, C. F., Ernst, M., Estaki, M., Fouquier, J., Gauglitz, J. M.,
477 Gibson, D. L., Gonzalez, A., Gorlick, K., Guo, J., Hillmann, B., Holmes, S., Holste, H.,
478 Huttenhower, C., Huttley, G., Janssen, S., Jarmusch, A. K., Jiang, L., Kaehler, B., Kang,
479 K. B., Keefe, C. R., Keim, P., Kelley, S. T., Knights, D., Koester, I., Kosciolek, T.,
480 Kreps, J., Langille, M. G., Lee, J., Ley, R., Liu, Y., Loftfield, E., Lozupone, C., Maher,
481 M., Marotz, C., Martin, B. D., McDonald, D., McIver, L. J., Melnik, A. V., Metcalf, J.
482 L., Morgan, S. C., Morton, J., Naimey, A. T., Navas-Molina, J. A., Nothias, L. F.,
483 Orchanian, S. B., Pearson, T., Peoples, S. L., Petras, D., Preuss, M. L., Pruesse, E.,
484 Rasmussen, L. B., Rivers, A., Robeson, I. I. M. S., Rosenthal, P., Segata, N., Shaffer,
485 M., Shiffer, A., Sinha, R., Song, S. J., Spear, J. R., Swafford, A. D., Thompson, L. R.,
486 Torres, P. J., Trinh, P., Tripathi, A., Turnbaugh, P. J., Ul-Hasan, S., Van der Hooft, J. J.,
487 Vargas, F., Vázquez-Baeza, Y., Vogtmann, E., Von Hippel, M., Walters, W., Wan, Y.,
488 Wang, M., Warren, J., Weber, K. C., Williamson, C. H., Willis, A. D., Xu, Z. Z.,
489 Zaneveld, J. R., Zhang, Y., Zhu, Q., Knight, R., Caporaso, J. G. (2018). QIIME 2:
490 Reproducible, interactive, scalable, and extensible microbiome data science. *PeerJ*
491 *Preprints*. 6:e27295v2 https://doi.org/10.7287/peerj.preprints.27295v2.

492

493 Chimienti, G., Piredda, R., Pepe, G., Werf, I. D. V. D., Sabbatini, L., Cecchio, C.,
494 Ricciuti, P., D'Erchia, A. M., Manzari, C., Pesole, G. (2016). Profile of microbial
495 communities on carbonate stones of the medieval church of San Leonardo di Siponto
496 (Italy) by Illumina-based deep sequencing. *Applied Microbiology and Biotechnology*,
497 100, 8537-8548. DOI: 10.1007/s00253-016-7656-8.
498
499 Costerton, J. W., Lewandowski, Z., Caldwell, D. E., Korber, D. R., Lappin-Scott, H. M.
500 (1995). Microbial biofilms. *Annual Review Microbiology*, 49, 11-45. DOI:
501 10.1146/annurev.mi.49.100195.003431.
502
503 Chukwujike, I. C., Igwe, I. O. (2016). Extender properties of some Nigerian clays.
504 *Journal of Minerals and Materials Characterization and Engineering*, 4, 279-291. DOI:
505 10.4236/jmmce.2016.45025.
506
507 Coutinho, M. L., Miller, A. Z., Gutierrez-Patricio, S., Hernadez-Marine, M., Gomez-
508 Bolea, A., Rogerio-Candelera, M. A., Philips, A. J. L., Jurado, V., Saizjimenez, C.,
509 Macedo, M. F. (2013). Microbial communities on deteriorated artistic tiles from Pena
510 National Palace (Sintra, Portugal). *International Biodeterioration & Biodegradation*,
511 84, 322-332. https://doi.org/10.1016/j.ibiod.2012.05.028.
512
513 Culman, S. W., Bukowski, R., Gauch, H. G., Cadillo-Quiroz, H., Buckley, D. H. (2009).
514 T-REX: software for the processing and analysis of T-RFLP data. *BMC Bioinformatics*,
515 171, 1-10. https://doi.org/10.1186/1471-2105-10-171.
516
517 Dias, D. S. B., Vasconcelos, U., Lutterbach, M. T. S., Cravo-Laureau, C., Sérvulo, E. F.
518 C. (2016). Sessile aerobic microbiota from the wall of the National Museum, Brazil:
519 characterization and quantification. *Canadian Journal of Pure & Applied Sciences*, 10,
520 3941-3949.
521
522 Dyda, M., Decewicz, P., Romaniuk, K., Wojcieszak, M., Sklodowska, A., Dziewit, L.,
523 Drewniak, L., Laudy, A. (2018). Application of metagenomic methods for selection of
524 an optimal growth medium for bacterial diversity analysis of microbiocenoses on
525 historical stone surfaces. *International Biodeterioration & Biodegradation*, 131, 2-10.
526 https://doi.org/10.1016/j.ibiod.2017.03.009.

Flemming, H. C., Wingender, J. (2001). Relevance of microbial extracellular polymeric substances (EPSs)--Part I: Structural and ecological aspects. *Water Science & Technology*, 43, 1-8. DOI: 10.2166/wst.2001.0326.

García-Esparza, J. A., Pardo, F., Palmero, L. M. (2017). A multi-analysis characterization of medieval and vernacular coating mortars in rural Valencia (Spain): An experimental study for a Heritage Action Plan. *Journal of Cultural Heritage*, 31, 83-96. https://doi.org/10.1016/j.culher.2017.10.013

Gaylarde, C. C., Baptista-Neto, J. A., Tabasco-Novelo, C., Ortega-Morales, O. (2018). Weathering of granitic gneiss: A geochemical and microbiological study in the polluted sub-tropical city of Rio de Janeiro. *Science of The Total Environment*, 644, 1641-1647. https://doi.org/10.1016/j.scitotenv.2018.07.303.

Gaylarde, C. C., Gaylarde, P. M. (2005). A comparative study of the major microbial biomass of biofilms on exteriors of buildings in Europe and Latin America. *International Biodeterioration & Biodegradation*, 55, 131-139. https://doi.org/10.1016/j.ibiod.2004.10.001.

Gaylarde, C. C., Morton, L. H. G., Loh, K., Shirakawa, M. A. (2011). Biodeterioration of external architectural paint films e a review. *International Biodeterioration & Biodegradation*, 65, 1189-1198. https://doi.org/10.1016/j.ibiod.2011.09.005.

Gaylarde, P. M., GAylarde, C. C. (1999). Algae and cyanobacteria on painted surfaces in Southern Brazil. *Revista de Microbiologia*, 30, 209-213. http://dx.doi.org/10.1590/S0001-37141999000300005.

Genhartdt, P., Murray, R. G. E., Wood, W. A., & Kieg, N. R. (1994). *Methods for general and molecular bacteriology*. (1st ed). Washington: American Society for Microbiology, (Section VI).

559 Gil, H., Calderón, J. A., Buitrago, C. P., Echavarría, A., Echevarría, F. (2010). Indoor
560 atmospheric corrosion of electronic materials in tropical-mountain environments.
561 *Corrosion Science*, 52, 327-337. https://doi.org/10.1016/j.corsci.2009.09.019.
562
563 Guerra, F. L., Lopes, W., Cazarolli, J. C., Lobato, M., Masuero, A. B., Molin, D. C. C.
564 D., Bento, F. M., Schrank, A., Vainstein, M. H. (2019). Biodeterioration of mortar
565 coating in historical buildings: Microclimatic Characterization, material, and fungal
566 community. *Building Environment*, 155, 195-209.
567 https://doi.org/10.1016/j.buildenv.2019.03.017.
568
569 Guillitte, O. (1995) Bioreceptivity: a new concept for building ecology studies. *The*
570 *Science of the Total Environment*, 167, 215–220. https://doi.org/10.1016/0048-
571 9697(95)04582-L.
572
573 Hartmann, M., Frey, B., Mayer, J., Mäder, P., Widmer, F. (2014). Distinct soil
574 microbial diversity under long-term organic and conventional farming. *The ISME*
575 *Journal*, 9, 1177-1194. DOI: 10.1038/ismej.2014.210.
576
577 Hernández, R. P. B., Pászti, Z., de Melo, H. G., Aoki, I. V. (2010). Chemical
578 characterization and anticorrosion properties of corrosion products formed on pure
579 copper in synthetic rainwater of Rio de Janeiro and São Paulo. *Corrosion Science*, 52,
580 826-837. https://doi.org/10.1016/j.corsci.2009.11.003.
581
582 Herrera, L. K., Videla, H. (2004). The importance of atmospheric effects on
583 biodeterioration of cultural heritage constructional materials. *International*
584 *Biodeterioration & Biodegradation*, 54, 125-134.
585 https://doi.org/10.1016/j.ibiod.2004.06.002.
586
587 Jurado, V., Miller, A. Z., Cuezva, S., Fernandez-Cortes, A., Benavente, D., Rogerio-
588 Candalera, M. A., Reyes, J., Cañaveras, J. C., Sanchez-Moral, S., Saizjimenez, C.
589 (2014). Recolonization of mortars by endolithic organisms on the walls of San Roque
590 church in Campeche (Mexico): A case of tertiary bioreceptivity. *Construction and*
591 *Building Materials*, 53, 348-359. https://doi.org/10.1016/j.conbuildmat.2013.11.114.
592

593 Lepinay, C., Mihajlovski, A., Touron, S., Seyer, D., Bousta, F., Martino, P. D. (2018).
594 Bacterial diversity associated with saline efflorescences damaging the walls of a French
595 decorated prehistoric cave registered as a world cultural heritage site. *International*
596 *Biodeterioration & Biodegradation*, 130, 55-64.
597 https://doi.org/10.1016/j.ibiod.2018.03.016.
598
599 Lutterbach, M. T. S., Oliveira, A. L. C., Zanatta, E. M., Costa, A. C. A. (2013). A
600 berlinda de aparato do imperador D. Pedro II: identificação de fungos em partes
601 selecionadas e sua relação com biodeterioração e aerobiologia. *Conservar Patrimônio*,
602 17, 59-72. DOI: 10.14568/cp2013003.
603
604 Manso, S., de Muynck, W., Segura, I., Aguado, A., Steppe, K., Boon, N., de Bilie, N.
605 (2014). Bioreceptivity evaluation of cementitious materials designed to stimulate
606 biological growth. *Science of The Total Environment*, 481, 232-241.
607 https://doi.org/10.1016/j.scitotenv.2014.02.059.
608
609 Mapelli, F., Morasco, R., Balloi, A., Rolli, E., Cappitelli, F., Daffinchio, D., Borin S.
610 (2012). Mineral-microbe, interactions: biotechnological potential of bioweathering.
611 *Journal of Biotechnology*, 157, 473-481. https://doi.org/10.1016/j.jbiotec.2011.11.013.
612
613 Marchesi, J. R., Sato, T., Weightman, A. J., Martin, T. A., Fry, J. C., Hiom, S. J., Wade,
614 W. G. (1998). Design and evaluation of useful bacterium-specific PCR primers that
615 amplify genes coding for bacterial 16S rRNA. *Applied environmental microbiology*, 64,
616 795–799.
617
618 Mihajlovski, A., Gabarre, A., Seyer, D., Bousta, F., Martino, P. D. (2017). Bacterial
619 diversity on rock surface of the ruined part of a French historic monument: The Chaalis
620 abbey. *International Biodeterioration & Biodegradation*, 120, 161-169.
621 https://doi.org/10.1016/j.ibiod.2017.02.019.
622
623 Miller, A. Z., Sanmartín, P., Pereira-Pardo L, Dionísio, A., Saiz-Jimenez, C., Macedo,
624 M. F. (2012). Bioreceptivity of building stones: A review. *Science of The Total*
625 *Environment*, 426, 1-12. https://doi.org/10.1016/j.scitotenv.2012.03.026
626

627 Mitchell, R., Gu, J. D. (2000). Changes in the biofilm microflora of limestone caused by
628 atmospheric pollutants. *International Biodeterioration & Biodegradation*, 46, 299-303.
629 https://doi:10.1016/S0964-8305(00)00105-0.
630
631 Nuhoglu, Y., Var, M., Koçak, E., Uslu, H., Demir, H. (2017). In Situ Investigation of
632 the biodeteriorative microorganisms lived on stone surfaces of the Sumela Monastery
633 (Trabzon, Turkey). *Journal of Environment Analytical Toxicology*, 7, 1-10.
634 https://doi10.4172/2161-0525.1000506.
635
636 Papida, S., Murphy, W., May, E. (2000). Enhancement of physical weathering of
637 building stones by microbial populations. *International Biodeterioration &*
638 *Biodegradation*, 46, 305-317. https://doi.org/10.1016/S0964-8305(00)00102-5.
639
640 Pédron J., Guyon L, Lecomte A., Blottière L., Chandeysson C., Rochelle-Newall E.,
641 Raynaud X., Berge O., Barny A-M. (2020). Comparison of environmental and culture-
642 derived bacterial communities through 16S Metabarcoding: a powerful tool to assess
643 media selectivity and detect rare taxa. *Microorganisms*, 8, 1129.
644 https://doi:10.3390/microorganisms8081129
645
646 Perez-Alvaro E. (2016). Climate change and underwater cultural heritage: Impacts and
647 challenges. *Journal of Cultural Heritage*, 21, 842-848.
648 https://doi.org/10.1016/j.culher.2016.03.006.
649
650 Piña R.G., and Cervantes C. (1996). Microbial Interactions with Aluminium. *Biometals,*
651 9, 311–316. https://doi.org/10.1007/BF00817932
652
653 Piotrowska-Seget, Z.; Cycoń, M.; Kozdrój, J. (2005) Metal-Tolerant Bacteria Occurring
654 in Heavily Polluted Soil and Mine Spoil. *Appl. Soil Ecol*., 28, 237–246. https://doi.org/
655 10.1016/j.apsoil.2004.08.001
656
657 Pitzurra, L., Morioni, B., Nocentini, A., Sbaraglia, G., Poli, G., Bistoni, F. (2003).
658 Microbial growth and air pollution in carbonate rock weathering. *International*
659 *Biodeterioration & Biodegradation*, 52, 63-68. https://doi.org/10.1016/S0964-
660 8305(02)00175-0.

661

662 Quast, C., Pruesse, E., Yilmaz, P., Gerken, J., Schweer, T., Yarza, P., Peplies, J.,
663 Glöckner, F. O. (2013). The SILVA ribosomal RNA gene database project: improved
664 data processing and web-based tools. *Nucleics Acids Research*, 41, 590-596.
665 https://doi:10.1093/nar/gks1219.

666

667 Quereda, J. J., Dussurget, O., Nahori, M. A., Ghozlane, A., Volant, S., Dillies, M. A.,
668 Regnault, B., Kennedy, S., Mondot, S., Villoing, B., Cossart, P., Pizarro-Cerda, J.
669 (2013). Bacteriocin from epidemic Listeria strains alters the host intestinal microbiota to
670 favor infection. *Proceedings of the National Academy of Sciences of the United States*
671 *of America*, 113, 5706-5711. https://doi.org/10.1073/pnas.1523899113.

672

673 Reeder, N. L., Kaplan, J., Xu, J., Youngquist, R. S., Wallace, J., Hu, P., Juhlin, K. D.,
674 Schwartz, J. R., Grant, R. A., Fieno, A., Nemeth, S., Reichling, T., Tiesman, J. P., Mills,
675 T., Steinke, M., Wang, S. L., Saunders, C. W. (2011). Zinc pyrithione inhibits yeast
676 growth through copper influx and inactivation of iron-sulfur proteins. *Antimicrobial*
677 *Agents and Chemotherapy*. 55, 5753-5760. Doi: 10.1128/AAC.00724-11.

678

679 Reis-Menezes, A. A., Gambale, W., Giudice, M. C. Shirakawa, M. A. (2011)
680 Accelerated testing of mold growth on traditional and recycled book paper.
681 *International Biodeterioration & Biodegradation,* 65, 423-428.
682 https://doi.org/10.1016/j.ibiod.2011.01.006.

683

684 Rittman, B. E., Pettis, M., Reeves, H. W., Stahl, D. A. (1999). How biofilm clusters
685 affect substrate flux and ecological selection. *Water Science and Technology*; 39, 99-
686 105. https://doi.org/10.1016/S0273-1223(99)00156-0.

687

688 Saddique, R., Chahal, N. K. (2011). Effect of ureolytic bacteria on concrete properties.
689 *Construction and Building Material*, 25, 3791-3801.
690 https://doi.org/10.1016/j.conbuildmat.2011.04.010.

691

692 Saiz-Jimenez, C. (1995). Deposition of anthropogenic compounds on monuments and
693 their effect on airborne microorganisms. *International Journal of Aerobiology*, 11, 161-
694 175. https://doi10.1007/BF02450035.

Sarró, M. I., García, A. M., Rivalta, V. M., Moreno D. A., Arroyo, I. (2006). Biodeterioration of the lions fountain at the Alhambra palace, Granada (Spain). *Building and Environment*, 41, 1811-1820. https://doi.org/10.1016/j.buildenv.2005.07.029.

Shirakawa, M. A., Gaylarde, C. C., Gaylarde, P. M., John, V., Gambale, W. (2002). Fungal colonization and succession on newly painted buildings and the effect of biocide. *FEMS Microbiology Ecology*, 39, 165-173. https://doi10.1111/j.1574-6941.2002.tb00918.x.

Shirakawa, M. A., John, V. M., Silva, M. E. S., Gaylarde, C. C. (2011). Biodeterioration of painted mortar surfaces in tropical urban and coastal situation: comparison of four paint formulations *International Biodeterioration & Biodegradation*, 65, 112-121. https://doi.org/10.1016/j.ibiod.2011.03.004.

Shirakawa, M. A., Tavares, R. G., Gaylarde, C. C., Taqueda, M. E. S., Loh, K., John, V. M. (2010). Climate as the most important factor determining anti-fungal biocide performance in paint films. *Science of the Total Environment*, 408, 5878-5886. https://doi10.1016/j.scitotenv.2010.07.084.

Shirakawa, M. A., Gaylarde, C. C., Sahão, H. D., Lima, J. R. B. (2013). Inhibition of Cladosporium growth on gypsum panels treated. *International Biodeterioration & Biodegradation*, 85, 57-61. https://doi.org/10.1016/j.ibiod.2013.04.018.

Silva, J. E. G., Mendonça, E. A. M., Gomes, U. V. R., Amaral, I. P. G., Arruda, R. R. A., Bonifacio, T. T. C. (2019). *Cobertura antifúngica à base de nanopartículas contendo piocianina*. BR 10 2019 016732 7.

Sogin, M. L., Gunderson, J. H. (1987). Structural diversity of eukaryotic small subunit ribosomal RNAs: evolutionary implications. *Annals of the New York Academy of Sciences* - NYAS Publications, 503, 125-139.

Stauffert, M. Cravo-Laureau, C., Jézéquel, R., Barantal, S., Cuny, P., Gilbert, F., Cagnon, C., Militon, C., Amouroux, D., Mahdaoui, F., Bouyssiere, B., Stora, G.,

729 Merlin, F., Duran, R. (2013). Impact of oil on bacterial community structure in
730 bioturbated sediments. *Plos One*, 8, 1-15. https://doi:10.1371/journal.pone.0065347.
731
732 Sterflinger, K., Ettenauer, J., Piñar, G. (2013). Bio-susceptibility of materials and
733 thermal insulation systems used for historical buildings. *Energy Procedia*, 40, 499-506.
734 https://doi.org/10.1016/j.egypro.2013.08.057.
735
736 Traversetti, L., Bartoli, F., Caneva, G. (2018). Wind-driven rain as a bioclimatic factor
737 affecting the biological colonization at the archaeological site of Pompeii, Italy.
738 *International Biodeterioration & Biodegradation*, 134, 31-38.
739 https://doi.org/10.1016/j.ibiod.2018.07.016
740
741 Vásquez-Nion, D., Silva, B., Prieto, B. (2018). Bioreceptivity index for granitic rocks
742 used as construction material. *Science of the Total Environment*, 633, 112-121.
743 https://doi10.1016/j.scitotenv.2018.03.171.
744
745 Viana, A. A. G., Martins, R. X., Ferreira, G. F., Zenaide Neto, H., Amaral, I. P. G.,
746 Vasconcelos, U. (2017) *Pseudomonas aeruginosa* and pyocyanin act negatively on the
747 establishment of *Enterobacteriacea* biofilm. *International Journal of Engineering*
748 *Research and Application*, 7, 23-30. DOI: 10.9790/9622-0708022330
749
750 Wang, Y., Qian, P. Y. (2009). Conservative fragments in bacterial 16S rRNA genes and
751 primer design for 16S ribosomal DNA amplicons in metagenomic studies. *PLOS ONE*,
752 4, 1-9. https://journals.plos.org/plosone/article?id=10.1371/journal.pone.0007401.
753
754 Wei, K. Y., Chen, Y. Y., Smolke, C. D. (2013). A yeast-based rapid prototype platform
755 for gene control elements in mammalian cells. *Biotechnology and Bioengineering*, 110,
756 1201-1210. https://doi10.1002/bit.24792.
757
758 Weisburg, W. G., Barns, S. M., Pelletier, D. A., Lane, D. J. (1991) 16S ribosomal DNA
759 amplification for phylogenetic study. *Journal of Bacteriology*. 173, 697-703. DOI:
760 10.1128/jb.173.2.697-703.1991
761

762 Wiktor, V., Grosseau, Ph., Guyonnet, R., Garcia-Diaz, E., Lors, C. (2011) Accelerated
763 weathering of cementitious matrix for the development of an accelerated laboratory test
764 of bio-deterioration. *Materials and Structures*. 44, 623-40.
765 https://doi.org/10.1617/s11527-010-9653-1.
766
767
768
769
770
771

772 Table 1. Deterioration and microbial density found in coupons after 100 days, in the *in situ* and in the inoculum samples. The values are
773 presented as mean ± SD (n=3).

Conditions/Pathology		**Ah***	**Ap-a†**	**Ib***	**Ah-f†**	**Ap-f†**	**F***	**Ph†**
In situ	-	$2.0 \pm 0.3 \times 10^{4}$	$1.0 \pm 0.1 \times 10^{3}$	$1.0 \pm 0.2 \times 10^{3}$	$5.0 \pm 0.1 \times 10^{4}$	$5.0 \pm 0.1 \times 10^{2}$	$5.0 \pm 0.2 \times 10^{3}$	$1.0 \pm 0.1 \times 10^{3}$
Inoculum	-	$1.0 \pm 0.1 \times 10^{10}$	-	$9.0 \pm 0.2 \times 10^{7}$	$1.0 \pm 0.1 \times 10^{8}$	-	$2.0 \pm 0.1 \times 10^{6}$	$6.0 \pm 0.1 \times 10^{4}$
1-CUW	Not significant	---	---	---	---	---	---	---
2-CCW	Not significant	---	---	---	---	---	---	---
3-CUA	Not significant	---	---	---	---	---	---	---
4-CCA	Not significant	---	---	---	---	---	---	---
5-MUW	Soft bulkier structure and robust biofilm	$5.7 \pm 0.2 \times 10^{6}$	$1.8 \pm 0.1 \times 10^{2}$	$6.0 \pm 0.3 \times 10^{4}$	$1.9 \pm 0.1 \times 10^{6}$	$1.4 \pm 0.1 \times 10^{4}$	$1.6 \pm 0.1 \times 10^{6}$	$9.4 \pm 0.5 \times 10^{4}$
6-MCW	Presence of cracks on surface coating, less biofilm and depigmentation	$4.8 \pm 0.2 \times 10^{4}$	$7.5 \pm 0.4 \times 10^{1}$	$3.5 \pm 0.3 \times 10^{3}$	$2.5 \pm 0.1 \times 10^{3}$	$5.0 \pm 0.1 \times 10^{-1}$	$1.9 \pm 0.1 \times 10^{3}$	NG
7-MUA	Adherent bulkier structure, large number of hyphae. Robust biofilm. Greenish and orange colonies.	$1.2 \pm 0.1 \times 10^{7}$	$1.8 \pm 0.1 \times 10^{2}$	$1.0 \pm 0.1 \times 10^{5}$	$5.6 \pm 0.2 \times 10^{6}$	$5.6 \pm 0.2 \times 10^{3}$	$7.0 \pm 0.4 \times 10^{4}$	$5.6 \pm 0.2 \times 10^{5}$
8-MCA	Presence of cracks on surface coating and paint changed to bright yellow, less biofilm and whitening. Greenish and orange colonies.	$3.6 \pm 0.2 \times 10^{6}$	$1.3 \pm 0.1 \times 10^{2}$	$5.1 \pm 0.2 \times 10^{4}$	$1.4 \pm 0.1 \times 10^{6}$	$3.1 \pm 0.05 \times 10^{0}$	$3.6 \pm 0.2 \times 10^{5}$	$3.1 \pm 0.1 \times 10^{0}$

774 Ah: Aerobic heterotrophic bacteria; Ap-a: aerobic acid-producing bacteria; Ib: Iron-oxidizing bacteria; Ah-f: facultative heterotrophic bacteria;
775 Ap-f: facultative acid-producing bacteria; F: Total fungi; Ph: Photosynthetic microorganisms. *(CFU/cm^2). †(MPN cells/cm^2); NG: no-growth.

776 Condition 1-CUW: Absence of microorganism, uncoated coupons and water mist; Condition 2-CCW: Absence of microorganism, coated
777 coupons and water mist; Condition 3-CUA: Absence of microorganism, uncoated coupons and acid mist; Condition 4-CCA: Absence of
778 microorganism, coated coupons and acid mist; Condition 5-MUW: Presence of microorganism, uncoated coupons and water mist; Condition 6-
779 MCW: Presence of microorganism, coated coupons and water mist; Condition 7-MUA: Presence of microorganism, uncoated coupons and acid
780 mist; Condition 8-MCA: Presence of microorganism, coated coupons and acid mist
781
782

783 Table 2. Alpha-diversity indexes of bacterial and fungal communities from the cultured
784 mortar treated with water mist (conditions 5 and 6) and acid mist (conditions 7 and 8)

Microbial group	Condition	# of ASVs	H'	D	Equitability
Bacteria	5 (uncoated)	21.00±1.70	2.68±0.60	0.75±0.14	0.61±0.15
	6 (coated)	13.00±3.60	1.13±0.25	0.36±0.09	0.31±0.05
	7 (uncoated)	42.30±9.10	3.28±0.27	0.82±0.05	0.61±0.05
	8 (coated)	14.30±5.50	1.09±1.28	0.29±0.36	0.27±0.28
Fungi	5 (uncoated)	7.00±0.00	1.90±0.37	0.65±0.15	0.68±0.13
	6 (coated)	7.33±2.08	1.26±0.04	0.49±0.01	0.44±0.07
	7 (uncoated)	9.67±2.52	2.09±0.44	0.68±0.12	0.65±0.14
	8 (coated)	7.67±0.58	1.24±0.72	0.42±0.27	0.42±0.24

785 Mean values and standard deviation of triplicates of each condition. ASVs, Amplicon
786 Sequence Variants; H', Shanon-Weaver's index; D, Simpson's index; Equitability,
787 Pielou's eveness.

Figure 1. Glass reactor (A) and top view of the arrangement of the coupons (B).

Figure 2. SEM image of the uninoculated (A) and inoculated (B) mortar coupons after 100 days of incubation. Conditions 2, 4, 6 and 8 represented coated mortar and 1, 3, 5 and 7 represented uncoated. Treatment with acid mist were used in conditions 3, 4, 7 and 8.

Figure 3. Image of mortar coupons at the beginning of the experiment (left, uncoated; right, coated), after 100 days of incubation and after scrapping off the biofilms. Conditions 2, 4, 6 and 8 represented coated mortar and 1, 3, 5 and 7 represented uncoated. Treatment with acid mist were used in conditions 3, 4, 7 and 8.

Figure 4. Bacterial (A) and Eukayotic (B) communities structures. Non-metric multidimensional scaling analysis (Bray-Curtis) based on T-RFLP profiles from 16S and 18S rRNA genes from biofilm developed in inoculated coupons under different conditions: uncoated coupons (C5 in green, condition 5-MUW), coated coupons (C6 in blue, condition 6-MCW), uncoated coupons under acid mist (C7 in cyan, condition 7-MUA) and coated coupons under acid mist (C8 in red, condition 8-MCA). The vectors connect the triplicates. The percentages indicate the average similarity (SIMPER) of samples in each group (condition).

Figure 5. Relative abundance of bacterial community at the genus level (A), fungal community at the class level (B) and ASVs distribution of the two dominants classes of Fungi (Sordariomycetes and Tremellomycetes) (C) in coated (conditions 5 and 7) and uncoated (conditions 6 and 8) mortar treated with water mist (conditions 5 and 6) and acid mist (conditions 7 and 8).


A
B

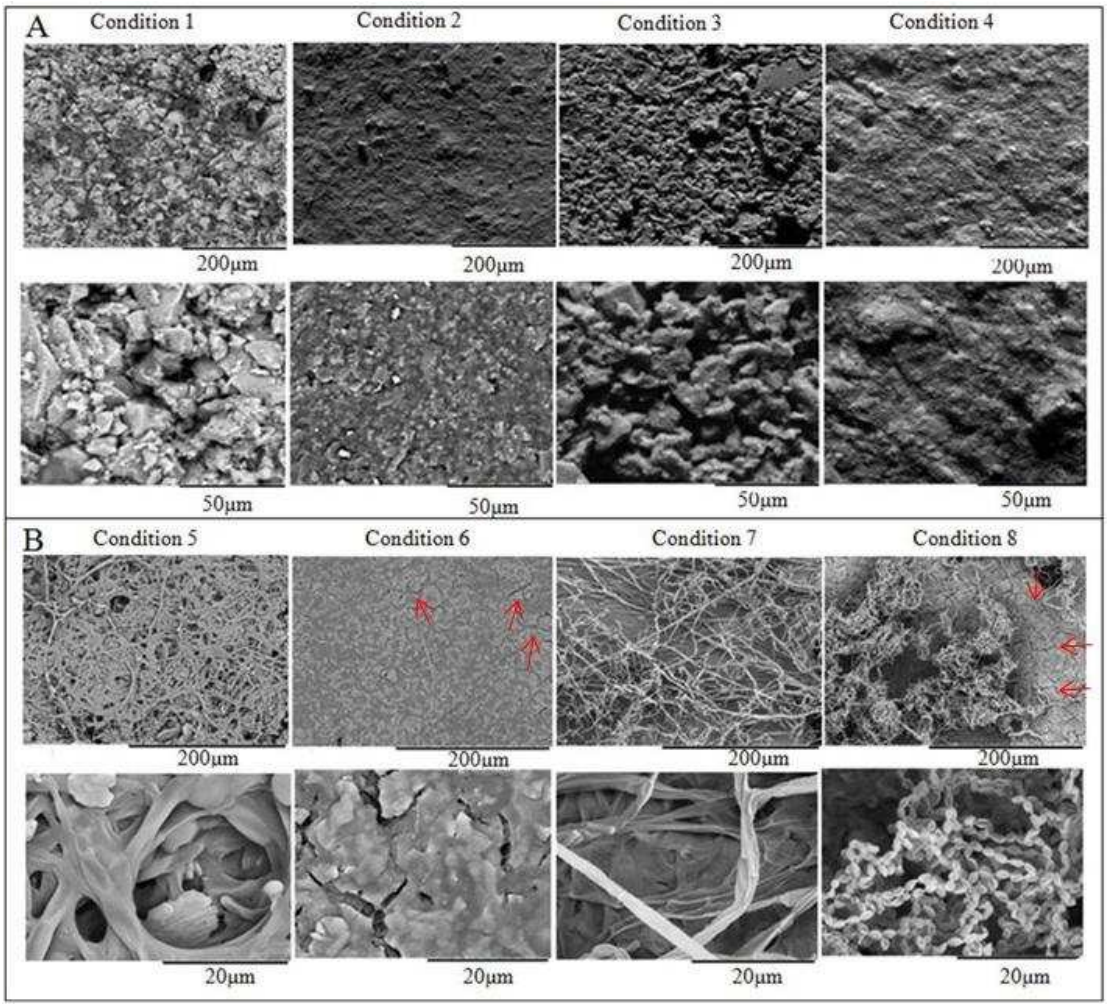
A
Condition 1
Condition 2
Condition 3
Condition 4
200μm
200μm
200μm
200μm
50μm
50μm
50μm
50μm
B
Condition 5
Condition 6
Condition 7
Condition 8
200μm
200μm
200μm
200μm
20μm
20μm
20μm
20μm

Initial Condition			
Condition 1 	Condition 2 	Condition 3 	Condition 4 
Condition 5 	Condition 6 	Condition 7 	Condition 8 
	After scrapping 		

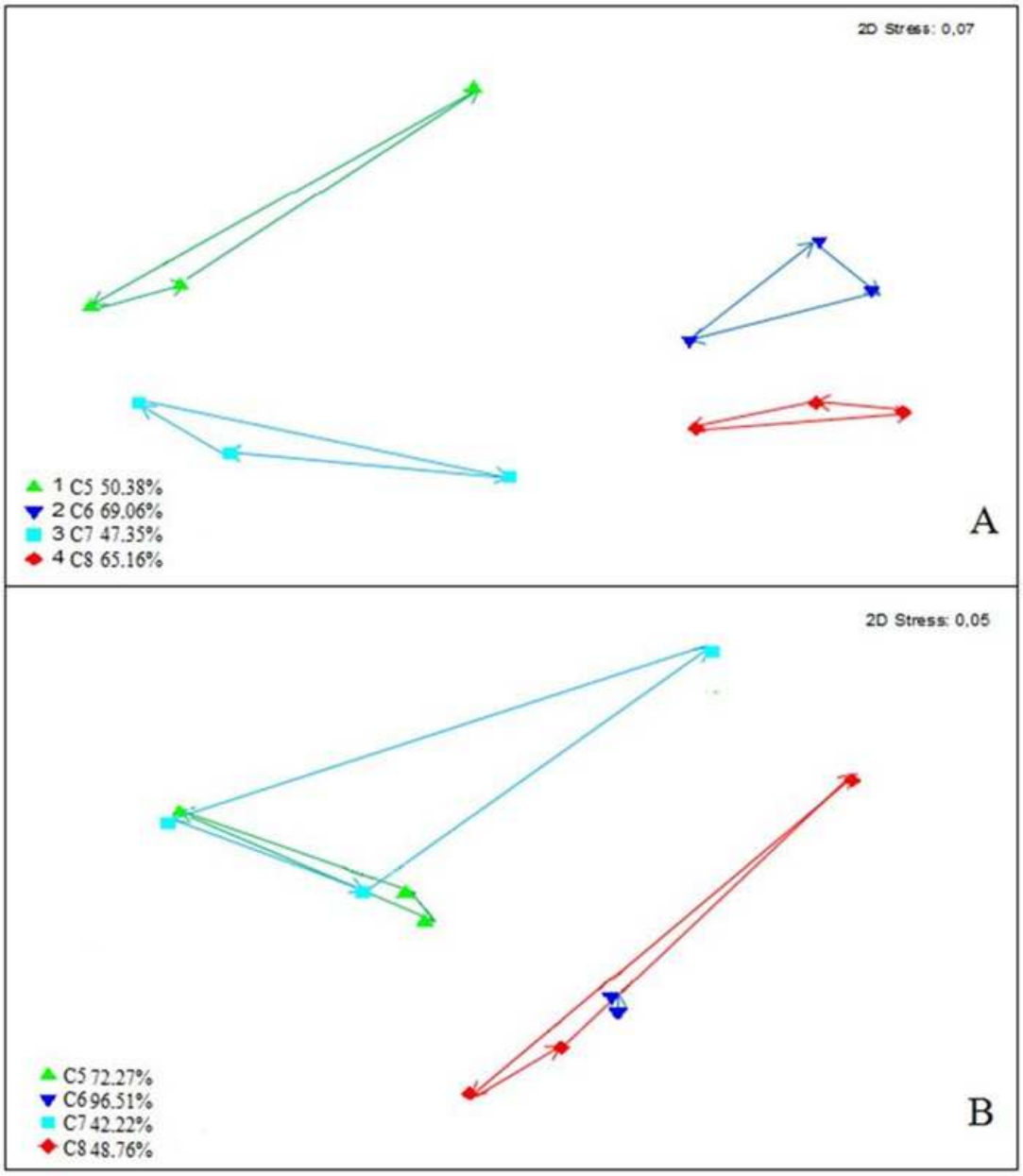
2D Stress: 0,07
1 C5 50.38%
2 C6 69.06%
3 C7 47.35%
4 C8 65.16%
A
2D Stress: 0,05
C5 72.27%
C6 96.51%
C7 42.22%
C8 48.76%
B

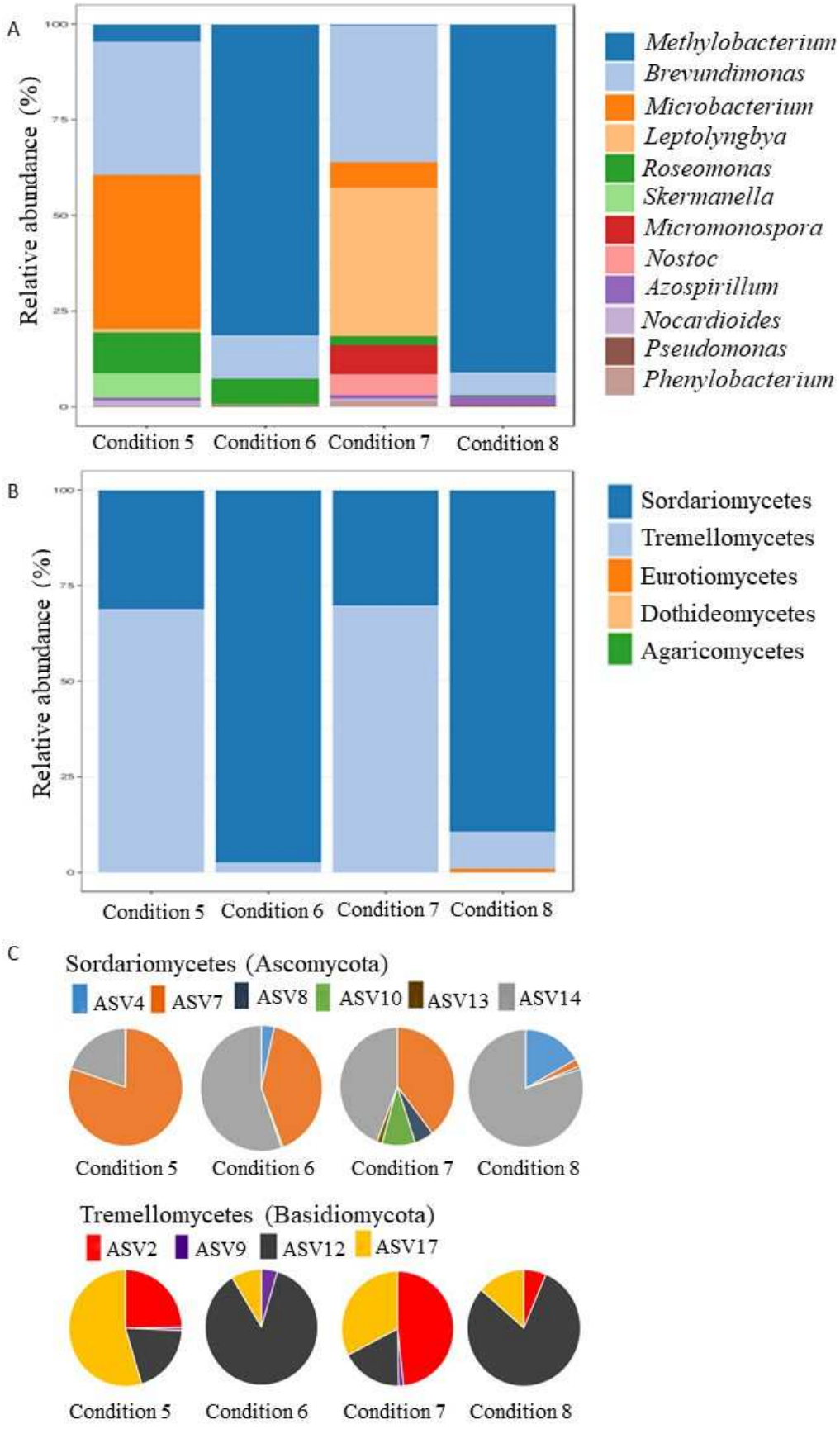
A
Relative abundance (%)
100
75
50
25
0
Condition 5
Condition 6
Condition 7
Condition 8
Methylobacterium
Brevundimonas
Microbacterium
Leptolyngbya
Roseomonas
Skermanella
Micromonospora
Nostoc
Azospirillum
Nocardioides
Pseudomonas
Phenylobacterium
B
Relative abundance (%)
100
75
50
25
0
Condition 5
Condition 6
Condition 7
Condition 8
Sordariomycetes
Tremellomycetes
Eurotiomycetes
Dothideomycetes
Agaricomycetes
C
Sordariomycetes (Ascomycota)
ASV4
ASV7
ASV8
ASV10
ASV13
ASV14
Condition 5
Condition 6
Condition 7
Condition 8
Tremellomycetes (Basidiomycota)
ASV2
ASV9
ASV12
ASV17
Condition 5
Condition 6
Condition 7
Condition 8

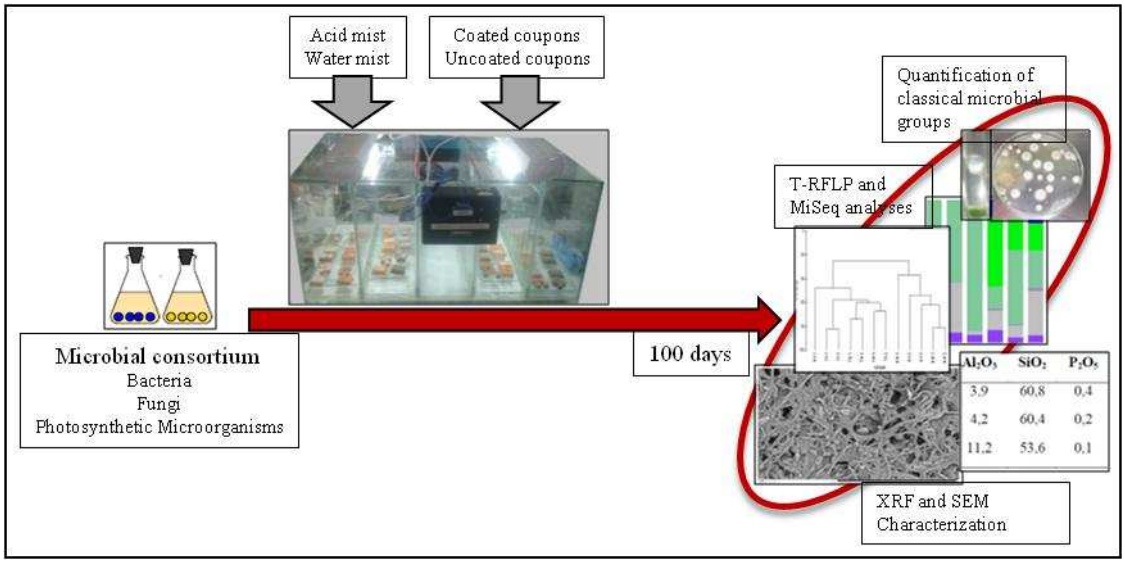
Acid mist
Water mist
Coated coupons
Uncoated coupons
Quantification of classical microbial groups
T-RFLP and MiSeq analyses
Microbial consortium
Bacteria
Fungi
Photosynthetic Microorganisms
100 days
Al_2O_3 SiO_2 P_2O_5
3,9 60,8 0,4
4,2 60,4 0,2
11,2 53,6 0,1
XRF and SEM Characterization